

## Highlights

- High water-application rates in centre-pivot systems can lead to soil erosion.
- Extent and severity of erosion underneath centre-pivots is currently unknown.
- We mapped erosion features in 738 centre pivots in Brazil using Google Earth™.
- We identified signs of erosion in 29% of the fields, with rill lengths up to 1200 m.
- We provide first evidence of widespread soil erosion under centre-pivot irrigation.

[Click here to view linked References](#)

1 **First evidence of widespread, severe soil erosion underneath centre-pivot**  
2 **irrigation systems**

3 Pedro V. G. Batista<sup>1</sup>, Victor B. da S. Baptista<sup>2</sup>, Florian Wilken<sup>1</sup>, Kay Seufferheld<sup>1</sup>,  
4 John N. Quinton<sup>3</sup>, Peter Fiener<sup>1</sup>

5 1 Water and Soil Resources Research, Institute of Geography, University of  
6 Augsburg, Augsburg, Germany

7 2 Department of Engineering, Federal University of Lavras, Lavras, Brazil

8 3 Lancaster Environment Centre, Lancaster University, Lancaster, UK

9 Correspondence to: Pedro V. G. Batista (pedro.batista@geo.uni-augsburg.de)

10 **Abstract**

11 Centre-pivot systems are widely used for irrigation in agriculture. However, excessive  
12 water application rates under low pressure centre-pivot systems can lead to soil  
13 erosion, which degrades soil structure and increases crop vulnerability to droughts.  
14 Although efforts have been deployed to measure soil erosion underneath individual  
15 centre-pivots, a large-scale systematic assessment of extent and severity of soil  
16 erosion in centre-pivot irrigated fields is currently lacking. Here we used Google  
17 Earth™ satellite images to provide first evidence of widespread, severe soil erosion  
18 in centre-pivot irrigated agricultural land. We focused on the municipality of Cristalina  
19 (6154 km<sup>2</sup>), in the Brazilian Central Highlands, where centre-pivots irrigate  
20 approximately 60 000 ha of cropland. The study area is in the Cerrado biome, which  
21 is one of the most important grain-producing regions in the world and Brazil's main  
22 centre-pivot irrigation area. By mapping erosion features under centre pivots, we  
23 found that 29% of centre-pivot fields displayed signs of rill erosion, with individual rills  
24 up to a length of 1200 m. Most erosion features were identified during the dry season

25 of the Brazilian Cerrado, which coincided with the period of greater satellite-image  
26 availability. Moreover, we found that compacted centre-pivot wheel tracks often  
27 triggered rill incision and that eroding centre-pivot fields displayed higher slope  
28 gradients and were better connected to surface waters than the non-eroding fields.  
29 Ultimately, the frequent identification of severe erosion features in the centre-pivot  
30 fields during the dry season indicates that irrigation causes and/or aggravates soil  
31 erosion in Cristalina and likely in other parts of the Brazilian Cerrado. This first  
32 systematic evidence of widespread soil erosion underneath centre-pivot systems  
33 highlights that irrigation erosion is an important but neglected driver of land  
34 degradation, and that urgent action is required to protect affected soils for future  
35 generations.

36 Keywords: erosion mapping; rill erosion; land degradation; Brazilian Cerrado; remote  
37 sensing; Google Earth™.

## 38 **1 Introduction**

39 For at least 5000 years, humankind has been developing irrigated agricultural  
40 systems to mitigate droughts and to increase crop production (Gulhati and Smith,  
41 1967). Currently 306 million ha (Mha) of land is under irrigation worldwide, with 240  
42 Mha of this land being converted from rainfed agriculture during the last century  
43 (1900 – 2005) (Siebert et al., 2015). The need for increased agricultural production  
44 and to deal with climate change are likely to further increase irrigated areas and  
45 efforts to save water and maximise irrigation efficiency (Puy et al., 2020; Rosa, 2022;  
46 Wang et al., 2021)

47 One approach to improving irrigation efficiency is to adopt centre-pivot irrigation  
48 systems. These systems are characterised by a moving lateral line with several  
49 emitters, supported above ground by towers that rotate around a central-pivot

50 mechanism, thus irrigating a circular area (Phocaides, 2000). They gained popularity  
51 during the second half of the 20<sup>th</sup> century, arguably due to their high efficiency,  
52 application uniformity, and low labour requirements (King, 2016). Currently, centre-  
53 pivot irrigation is found in some of the main cereal-producing countries of the world  
54 and is the preferred irrigation method in the USA (King, 2016) and Brazil (ANA,  
55 2021). Centre-pivot systems are also being increasingly employed for irrigation in  
56 Argentina, China, Portugal, Saudi Arabia, and Spain (Aimar et al., 2022; Johansen et  
57 al., 2021; Lian et al., 2022; Silva, 2017).

58 Centre pivots are often run at low pressure in order to reduce energy demands and  
59 decrease operational costs (Baptista et al., 2019). However, lowering the pressure of  
60 the centre-pivot systems leads to increased water application rates, due to a  
61 decrease in the wetted perimeter of the spray area and an increase in droplet size  
62 (Gilley, 1984; Hasheminia, 1994).

63 Peak application rates in low pressure centre-pivot systems can reach 200 mm h<sup>-1</sup>  
64 (King and Bjorneberg, 2011), which exceeds the intensity of most natural rainfall  
65 events. Application of water at high intensity leads to infiltration-excess runoff  
66 generation, even in highly permeable soils (Hasheminia, 1994; Kincaid, 2002) and it  
67 is recognised that runoff and soil erosion can be a significant problem under centre  
68 pivots (Kincaid, 2005, 2002; King, 2016; King and Bjorneberg, 2011; Silva, 2017,  
69 2006). Soil erosion in irrigated arable land is particularly problematic because soil  
70 degradation resulting from erosional processes can reduce water holding capacity  
71 and therefore exacerbate crop vulnerability to droughts (Batista et al., 2023b; Quinton  
72 et al., 2022), which in turn might increase irrigation demands through a positive  
73 feedback loop. However, despite the recognition that erosion is a problem under  
74 centre pivots, research to date has been based on individual field studies where (i)

75 soil and water losses were measured from experimental plots during irrigation (King,  
76 2016; King and Bjorneberg, 2011), and (ii) different management techniques to  
77 minimise runoff and soil erosion were tested at the plot scale (Kincaid et al., 1990;  
78 Silva, 2017). This means that there is a lack of systematic information regarding the  
79 extent and severity of soil erosion in centre-pivot-irrigated land worldwide.

80 Erosion mapping, where erosion and depositional features are identified from aerial  
81 and/or satellite images, offer the best option for e assessing the frequency and  
82 severity of erosion under centre pivots; and has previously been used in agricultural  
83 land over time and across large areas (Fischer et al., 2018; Zweifel et al., 2019).  
84 Nevertheless, timing of the images compared to the occurrence of erosion events  
85 can be a problem as tillage and crop growth can mask erosion features (Boardman,  
86 2016). Modelling offers an alternative approach and erosion models can be suitable  
87 for identifying eroding fields at regional scale, provided that models are fit for purpose  
88 and that adequate data is available for parameterisation (Batista et al., 2019).  
89 However, to our knowledge there is no model able to reliably simulate soil erosion  
90 under centre-pivot systems (see Kincaid, 2002), which ruled out this approach.

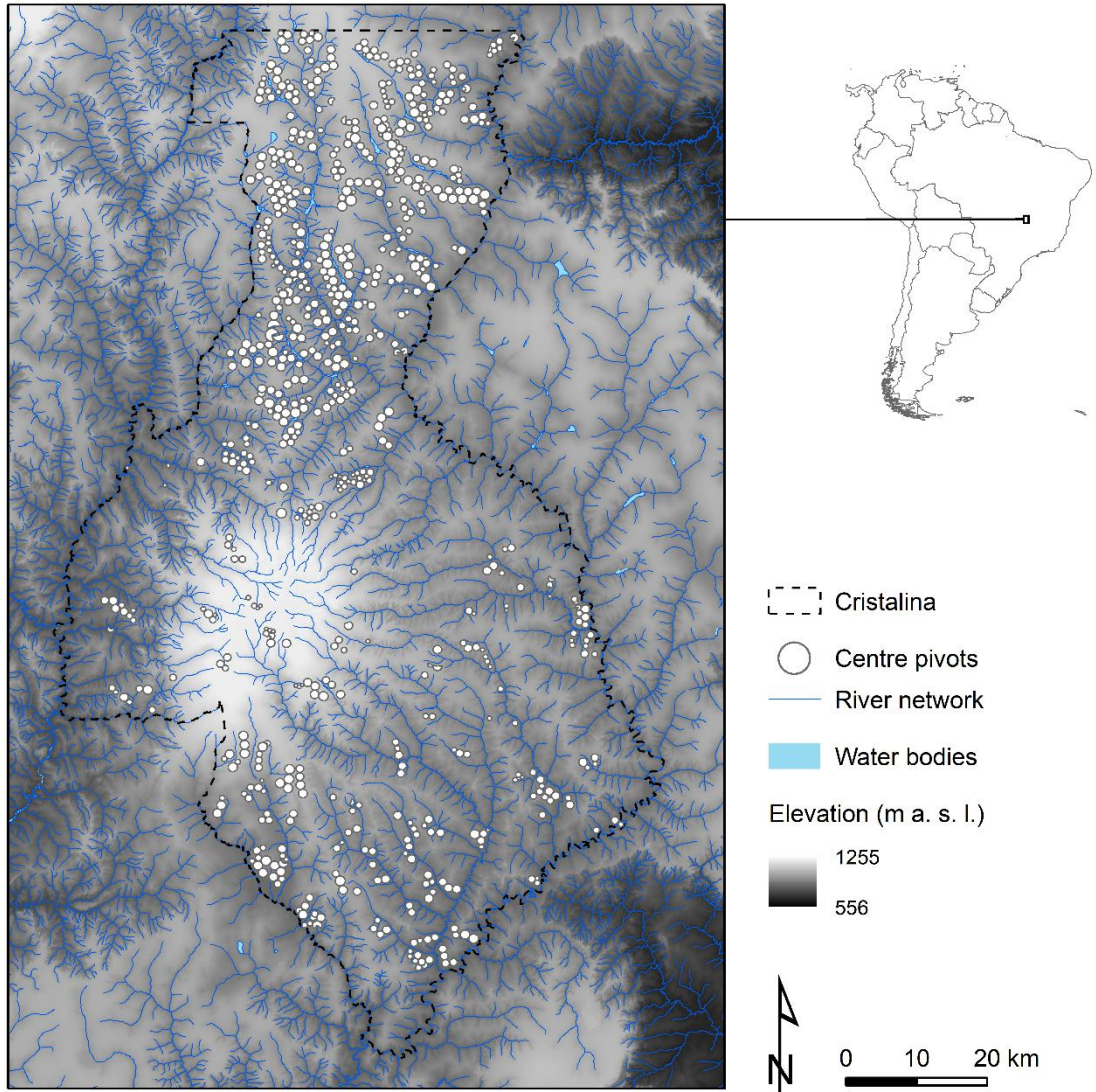
91 Here we investigate the presence and severity of soil erosion underneath centre-pivot  
92 irrigation systems using high-resolution satellite images from Google Earth™ (GE).  
93 The intensity and frequency of erosion features in 738 centre-pivot fields in the  
94 municipality of Cristalina (6154 km<sup>2</sup>), state of Goiás, Brazil were mapped. The study  
95 area was chosen due to its importance for irrigated cereal production in Brazil and  
96 due to the availability of multiple GE images over time. Moreover, the centre-pivot  
97 fields in Cristalina represent the cropping systems, soil types, and slope gradients  
98 typically found in the Brazilian Cerrado, one of the most important grain-producing  
99 regions of the world and the main centre-pivot irrigated zone in Brazil. Importantly,

100 the climate in the region is characterised by a pronouncedly dry winter, which helps  
101 to differentiate erosion features associated with either rainfall or irrigation. To the best  
102 of our knowledge, this study presents the first systematic, broad assessment of soil  
103 erosion severity under centre-pivot irrigation systems.

## 104 **2 Methods**

### 105 **2.1 Study area**

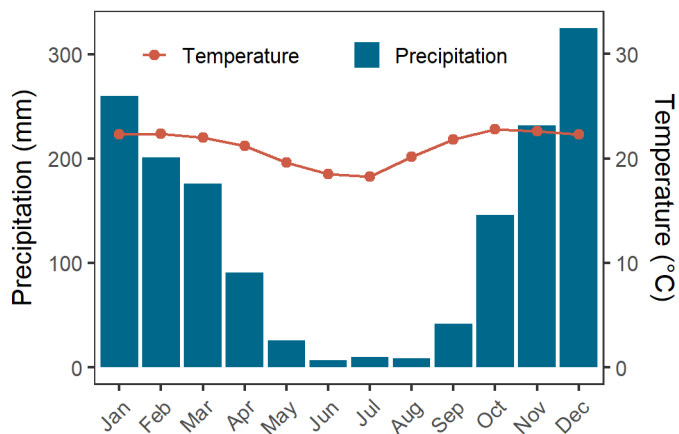
106 The municipality of Cristalina, state of Goiás, covers an area of 6154 km<sup>2</sup> in the  
107 Brazilian Central Highlands (Figure 1). The region is part of the Cerrado biome, which  
108 is characterised by a savannah-like vegetation and a markedly seasonal tropical  
109 climate, with rainy summers and dry winters (Aw climate type in Köppen's climatic  
110 classification). The average monthly temperature in Cristalina is 21 °C and the  
111 average annual precipitation is 1524 mm, which is almost entirely concentrated in the  
112 rainy season (September-April) (Alvares et al., 2013) (Figure 2).



113

114 Figure 1. Digital elevation model (DEM), hydrography, and centre-pivot irrigated fields  
 115 in the municipality of Cristalina, Brazil.

116



117

118 Figure 2. Long-term average monthly temperature and rainfall (1950-1990) for the  
 119 municipality of Cristalina, Brazil. Data from Alvares et al. (2013).

120 Elevation in Cristalina ranges from 732 to 1255 m a.s.l. (median = 910 m a.s.l.)  
 121 (Figure 1). Slopes are mostly gentle (median = 6%; interquartile range = 3 – 9%),  
 122 coinciding with the occurrence of deeply weathered-leached Ferralsols, on the  
 123 highest positions of the landscape, and Plinthosols, on hillsides and tableland edges  
 124 (EMATER, 2016, Marques et al., 2004). Cambisols are found on steeper terrain at  
 125 the edge of Tertiary erosional surfaces (Marques et al., 2004). The eastern side of  
 126 the municipality is drained by the São Marcos River, whilst the western area is  
 127 drained by the Corumbá River, both of which are part of the Paraná basin.

128 Land use in Cristalina is characterised by an intensive agriculture, which expanded  
 129 into the Brazilian Cerrado in the second half of the 20<sup>th</sup> century. This resulted in the  
 130 conversion of low fertility soils to crop production by liming and high fertiliser input  
 131 (Lopes and Guilherme, 2016). Currently, the Cerrado region is one of most important  
 132 grain-producing areas in the world and arguably Brazil's most threatened biome  
 133 (Garrett et al., 2018; Hunke et al., 2015). In Cristalina, permanent and annual  
 134 cropland occupy about 34% of the municipality area (IBGE, 2017). As in most of the  
 135 Cerrado, the main harvested crops are soyabeans (*Glycine max*), maize (*Zea mays*),



136 and common beans (*Phaseolus vulgaris*) (IBGE, 2017). Importantly, Cristalina is in  
137 the main centre-pivot irrigation zone of Brazil and is the municipality with the third  
138 largest centre-pivot irrigated area in the country, with 783 pivots that irrigate an area  
139 of approximately 60 000 ha (mean irrigated area per centre pivot is 76 ha) (ANA,  
140 2021).

141 Year-round use of centre-pivot systems means that soils are not only exposed to  
142 erosive water drops in the rainy season, but throughout the year. Centre-pivot  
143 irrigation in Cristalina (and throughout the Brazilian Cerrado) allows for 4-5 crops for  
144 every two crop years, with a typical crop rotation of soyabeans (1<sup>st</sup> crop, sowed in  
145 Sep/Oct) followed by maize (2<sup>nd</sup> crop, sowed in Jan/Feb/Mar), potentially followed by  
146 common beans (3<sup>rd</sup> crop, sowed in Apr/May) (ANA, 2021). Irrigation is used to  
147 supplement water deficits for the 1<sup>st</sup> crop in the case of dry spells during summer; to  
148 increase productivity for the 2<sup>nd</sup> crop, which is partially grown during the dry season;  
149 and to irrigate the third crop, which relies almost entirely on irrigation water (ANA,  
150 2021).

## 151 **2.2 Classification of erosion features**

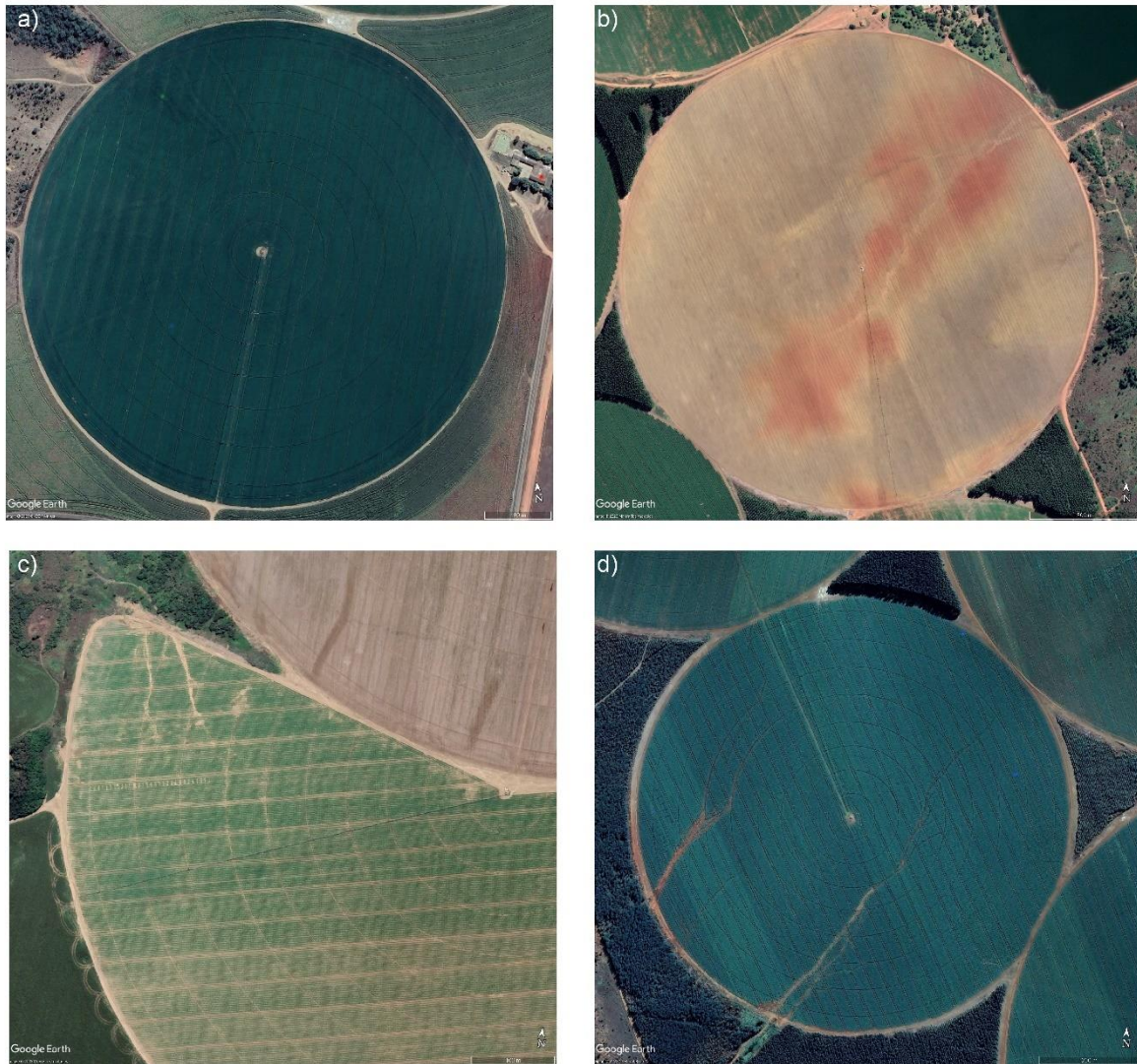
152 To assess the severity and extent of soil erosion underneath centre pivots in  
153 Cristalina, we examined high-resolution satellite images available from Google  
154 Earth™ (GE). These images are free to access and allow for the identification of  
155 erosion features, such as rills and ephemeral gullies, with comparable results to field-  
156 mapped data (Boardman, 2016). The location of each centre-pivot in the study area  
157 was taken from the Brazilian Irrigation Atlas (ANA, 2021), which used multiple  
158 satellite images to identify centre-pivot fields in Brazil for the year of 2019.

159 Our approach consisted of ranking erosion severity classes based on a visual  
160 interpretation of erosion features (Fischer et al., 2018). Since the timing of GE

161 images is somewhat arbitrary and spatially heterogeneous, we decided to analyse  
162 the last five images available for the location of each centre-pivot field. Hence, the  
163 image dates and the number of available images may vary between individual fields.  
164 To reduce the potential for misclassifications, we did not consider depositional  
165 features, interrill erosion, or signs of soil truncation. Instead, we focused on  
166 identifying linear erosion features, which are more easily distinguishable in the  
167 images. For simplicity, hereon these linear features will be referred as erosion rills,  
168 although some might be considered ephemeral gullies.

169 As such, we predefined four erosion classes:

- 170 • Class 0: no visible erosion rills underneath the centre-pivot area (Figure 3a).
- 171 • Class 1: legacy rills still visible after tillage, harvest, or crop growth; not  
172 actively eroding at the time of the image (Figure 3b).
- 173 • Class 2: visible, active rills with a maximum length shorter than  $\frac{1}{4}$  of the pivot  
174 diameter; rill-affected area less than 25% of the field area (Figure 3c).
- 175 • Class 3: visible, active rills with a maximum length longer than  $\frac{1}{4}$  of the pivot  
176 diameter; or rill-affected area greater than 25% of the field area (Figure 3d).



177

178 Figure 3. Classification example: a) Centre-pivot field (Jun 2021) with no signs of rill  
 179 erosion (Class 0); b) Centre-pivot field (May 2020) with legacy signs of rill erosion  
 180 (Class 1); c) Centre-pivot field (May 2019) with longest rill  $< \frac{1}{4}$  of the pivot diameter  
 181 (Class 2); d) Centre-pivot image (July 2019) with longest rill  $> \frac{1}{4}$  of the pivot diameter  
 182 (Class 3). Imagery from Google Earth™.

183 In August 2022, one classifier (Classifier #1, trained researcher in soil erosion)  
 184 performed an initial classification of all centre-pivot fields, using the latest available  
 185 images in GE, as described above. This same classifier then reanalysed all the  
 186 centre-pivot field images with the presence of erosion features (Classes  $> 0$ ), this

187 time measuring the length of the longest rill per centre-pivot image and correcting for  
188 false positives. From October to December 2022, two additional classifiers (Classifier  
189 #2 and Classifier #3, trained researchers in soil erosion) accomplished another  
190 classification of all centre-pivot fields (25% of the pivots by Classifier #2, 75% of the  
191 pivots by Classifier #3). This was performed to evaluate the agreement between the  
192 classifiers and to provide an assessment of classification error, which was quantified  
193 by a confusion matrix, Cohen's kappa coefficient, and the root mean square deviation  
194 (RSMD) of the categorisations (Classes 0 to 3). Of note is that the additional  
195 classifiers were also responsible for identifying the presence of soil conservation  
196 structures (e.g., broad-based terraces and grassed waterways), offsite pollution-  
197 control structures (e.g., road and in-field retention basins), and potential triggers for  
198 rill incision (e.g., compacted tramlines, Saggau et al. 2022, Silgram et al. 2010) in the  
199 centre-pivot fields. Moreover, to interpret the classification outputs we used terrain  
200 attributes (slope gradient and flow distance to the nearest stream channel) derived  
201 from a 30 m x 30 m resolution digital elevation model (DEM) from the Shuttle Radar  
202 Topography Mission (SRTM).

### 203 **3 Results and Discussion**

#### 204 **3.1 Classification of erosion features in centre-pivot fields and its accuracy** 205 **assessment**

206 We classified 738 from the 783 centre-pivot fields mapped in Cristalina by the  
207 Brazilian Irrigation Atlas (ANA, 2021) (total area = 56 462 ha). The remaining fields  
208 (45) could not be identified by at least one of the classifiers during the image  
209 analysis, e.g., the pivots were not present when the GE images were taken.

210 Approximately four images per centre-pivot field were analysed. Thus, a total of 2950  
211 centre-pivot-field images were analysed by Classifier #1 and 2966 by Classifiers #2

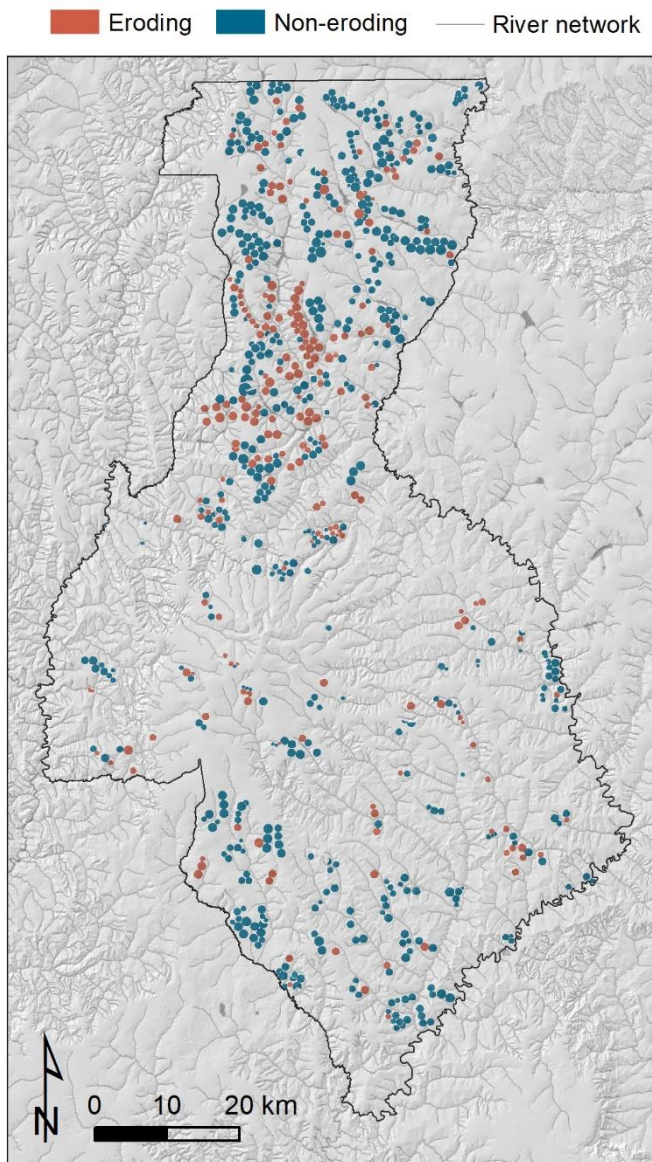
212 and #3, combined. The slightly larger number of centre-pivot-field images analysed  
213 by the Classifiers #2 and #3 was explained by the availability of more recent GE  
214 images when they performed their classification, which led to a difference in the  
215 dates of the images analysed by the classifiers. For instance, Classifiers #2 and #3  
216 analysed 62 centre-pivot-field images from 2022, while only one field-image from this  
217 year was evaluated by Classifier #1. Accordingly, the median period covered by the  
218 GE images per centre-pivot field was three years, for Classifier #1, and four years for  
219 Classifiers #2 and #3. In both cases the median year of the images per centre-pivot  
220 field was 2019.

221 To estimate the agreement between classifiers, 2188 centre-pivot-field images were  
222 classified twice. Classifiers #2 and #3 identified signs of erosion in 331 centre-pivot  
223 fields (Class > 0 for at least one of the available GE images). Classifier #1 was more  
224 conservative identifying 238 eroding fields, possibly due to the additional  
225 classification performed during the measurement of rill lengths (see section 2.2). The  
226 identification of centre-pivot fields with the presence of erosion features had an  
227 overall agreement between classifiers of 80% (76% for non-eroding fields and 87%  
228 for eroding fields) (Cohen's kappa = 0.59). The differences between the classifiers  
229 stemmed from missing small signs of rill erosion, mistaking cattle trails for rills, and  
230 potential typing errors when tabulating the data. The longer period covered by the GE  
231 images per centre-pivot field available for Classifiers #2 and #3 might have also  
232 increased their identification of centre-pivot-field images with erosion features.

233 According to the matching classifications, 211 centre-pivot fields displayed signs of  
234 rill erosion, which corresponded to 29% of 738 analysed fields (Figure 4). The  
235 eroding centre-pivot fields were more likely to be identified when a larger number of  
236 images from different timepoints were available (Figure 5). This highlights the



237 importance of the timing of the image corresponding with period of erosion events  
238 when identifying erosion features (Boardman, 2016; Fischer et al., 2018). It also  
239 points out that our approach underestimates the number of eroding fields for the  
240 areas with fewer images.

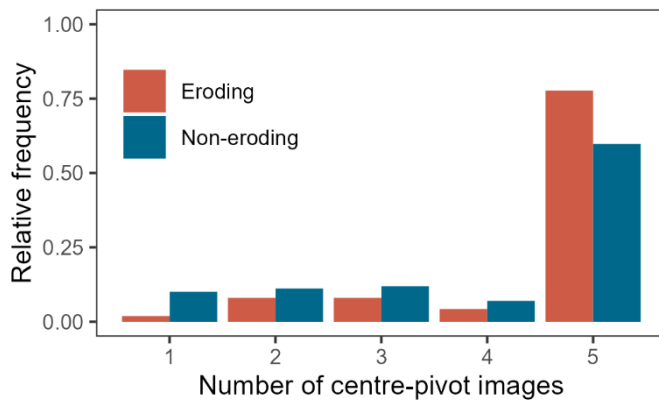


241

242 Figure 4. Location of eroding and non-eroding centre-pivot fields in Cristalina, Brazil.

243 Only those fields where both classifiers identified erosion features were considered to

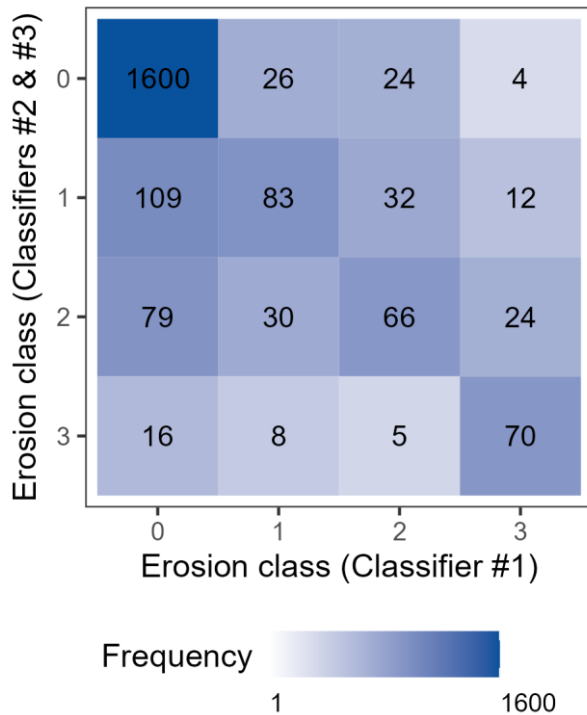
244 be eroding.



245

246 Figure 5. Relative frequency (0 – 1) of the number of GE images per centre-pivot field  
 247 for eroding and non-eroding fields.

248 If we considered only the 2188 centre-pivot-field images with matching image dates,  
 249 it was clear that the disagreements between classifiers were mostly associated to the  
 250 assignment of neighbouring categories (Cohen's kappa = 0.53; RMSD = 0.24)  
 251 (Figure 6). This pattern was particularly evident for erosion classes 1 and 2, which  
 252 displayed the lowest classification agreement (74% and 72%, respectively). The  
 253 discrepancies in these classes were expected, as the identification of smaller rills is  
 254 error prone. Moreover, distinguishing what constitutes a legacy rill, compared to an  
 255 actively eroding one, is partially subjective. Nevertheless, Classifier #1 assigned a  
 256 greater proportion of eroding centre-pivot images to Class 3 (29%) and a lesser  
 257 proportion to Classes 1 and 2 (38% and 33%, respectively), compared to Classifiers  
 258 #2 and #3 (Class 1 = 44%, Class 2 = 37%, Class 3 = 19%) (Figure 6).



259

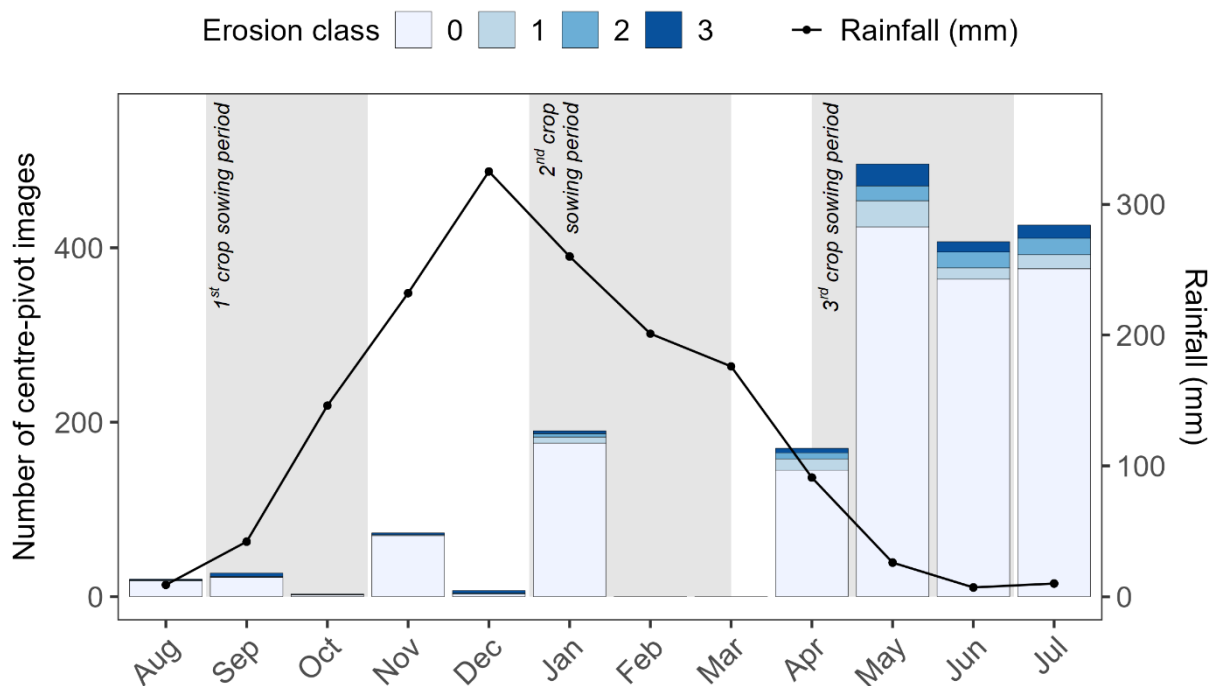
260 Figure 6. Confusion matrix for the erosion-feature classes assigned by Classifier #1  
 261 and Classifiers #2 and #3 for the centre-pivot-field images. Numbers in the boxes  
 262 refer to the frequency of erosion classes assigned by the classifiers.

263 To increase the confidence in our soil erosion assessment, we focused the remainder  
 264 of our results and discussion on the centre-pivot fields and centre-pivot-field images  
 265 where classifications agreed. A shapefile containing the location of the centre-pivot  
 266 fields, their erosion classification, and the date of the analysed GE images have been  
 267 uploaded to an open-access data repository (Batista et al., 2023a). Moreover, in the  
 268 following sections we provide a centre pivot identification number (Pivot ID) for all  
 269 figures which display GE images of centre-pivot fields. This number is taken from the  
 270 Brazilian Irrigation Atlas (ANA, 2021) and can be used to identify the centre-pivot  
 271 fields in the above-mentioned shapefile.

272 **3.2 Temporal patterns of soil erosion in centre-pivot irrigated fields**



273 Most erosion features were identified during the dry season of the Brazilian Cerrado,  
 274 using images from May, June, and July (Figure 7). This was related to the greater  
 275 availability of GE images with low cloud cover during this period of the year. Erosion  
 276 features were identified in more than one image for 52% of the centre-pivot fields.  
 277 This frequent identification of active, severe signs of rill erosion during periods with  
 278 very low rainfall indicates that centre-pivot irrigation might be either aggravating or  
 279 initiating soil erosion. As argued by Boardman and Evans (2020), the timing of  
 280 erosion monitoring is critical, as erosion signs are easily be masked by vegetation –  
 281 particularly in the humid tropics.

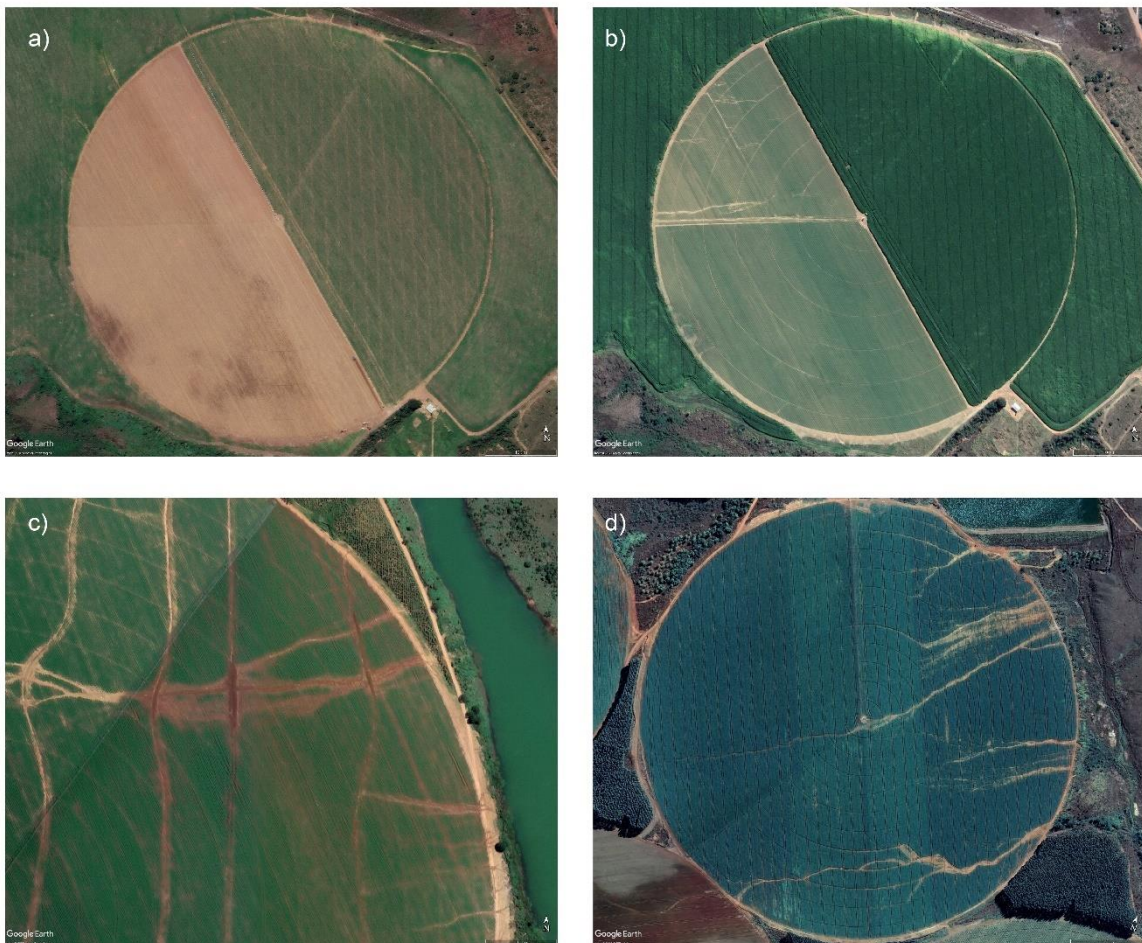


282

283 Figure 7. Number of analysed centre-pivot fields according to the month of the year  
 284 of the GE images. Rainfall data from Alvares et al. (2013).

285 As rills incised during the rainy season would have been at least partially filled up  
 286 during tillage, harvesting, and sowing of the subsequent crops (Figure 8a), the  
 287 erosion features identified in the months of May to July are likely to be associated

288 with the second or third crop in the rotation. Active erosion features (Classes 2 and 3)  
289 associated with the third crop (typical sowing dates from April to May), provide  
290 evidence that irrigation is the driver of soil erosion underneath the centre-pivots  
291 (Figure 8b). In cases where active rills were found in the second crop, we cannot  
292 disregard the hypothesis that the channels were already established by rainfall  
293 erosion at the end of the rainy season, which coincides with the sowing dates (Figure  
294 7) and the early development stages of the second crop. However, the severity and  
295 extent of the soil erosion features identified during the height of the dry season  
296 indicate that, at the very least, irrigation is partially responsible for the activity of rills  
297 (Figure 8d). There is also evidence that centre-pivot irrigation promoted soil erosion  
298 in previously established rill channels (Figure 8c).



300 Figure 8. a) Freshly tilled soil in a centre-pivot field in April 2020 (Pivot ID 17149,  
301 diameter = 620 m). b) Soil erosion for the same field (Pivot ID 17149) in May 2020:  
302 rills initiated from the centre-pivot circular wheel tracks, as seen on the top-left  
303 centre-pivot quadrant, and from a linear feature leading to the pivot. c) Soil erosion  
304 during centre-pivot irrigation in April 2018: darker-red (wet) soil can be seen moving  
305 along the rills and being deposited on adjacent dirt roads while the irrigation tower  
306 moves counter clockwise (Pivot ID 16629, diameter = 1370 m). d) Extensive rill  
307 network across the centre-pivot-field diameter in July 2019 (Pivot ID 11705, diameter  
308 = 1115 m); breached circular centre-pivot wheel tracks lead to rill incision, parallel  
309 tracks supply sediment and runoff to the incised rill network. Imagery from Google  
310 Earth™.

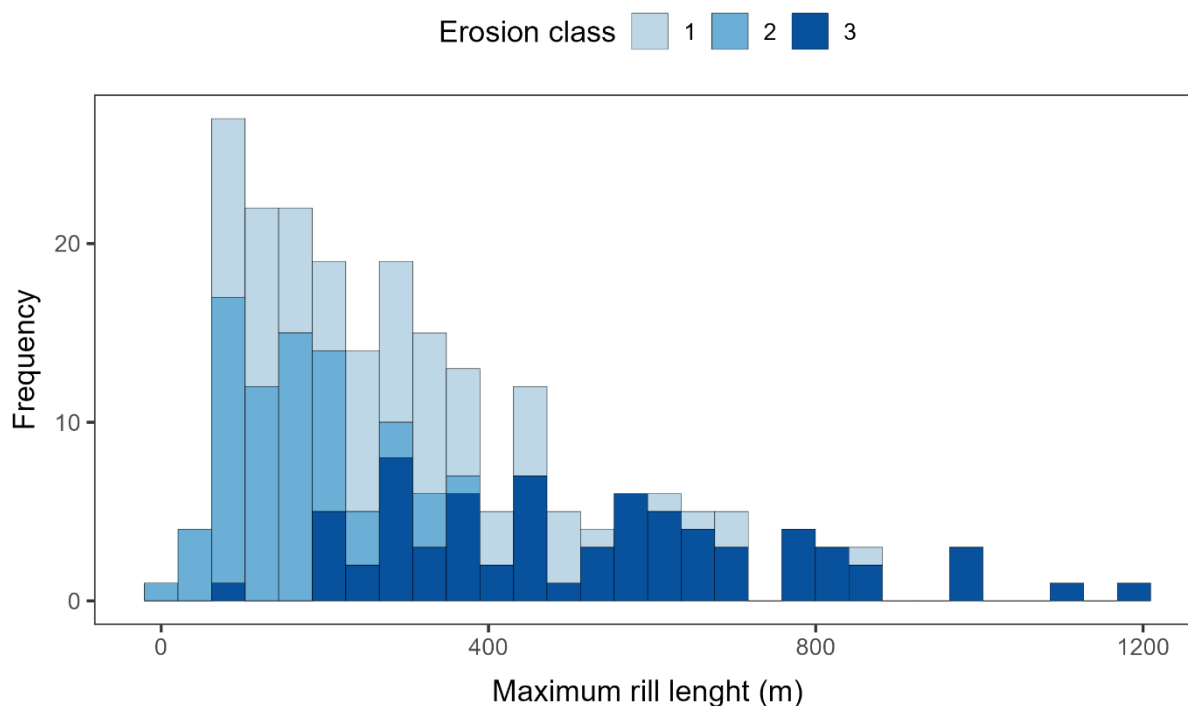
311 The occurrence of erosion under centre pivots can be attributed to the water  
312 application rates, which typically reach 60 to 200 mm hr<sup>-1</sup> (King and Bjorneberg,  
313 2011). Such application rates are likely to exceed many of the soil infiltration  
314 capacities in the region (around 50 mm hr<sup>-1</sup> for Ferralsols in the Cerrado, Barcelos et  
315 al., 1999; Panachuki et al., 2011) and lead to overland flow and soil erosion.  
316 Moreover, on top of directly causing soil erosion, rill incision was also triggered due to  
317 the breaching of compacted centre-pivot wheel tracks (Figure 8b,d).

### 318 **3.3 Extent and drivers of soil erosion in centre-pivot-irrigated fields**

319 The median length of the longest rill per centre-pivot image was 260 m (interquartile  
320 range = 151 – 440 m), with a maximum value over 1200 m (Figure 9). These rill  
321 lengths are some of the longest described in the scientific literature and exceed those  
322 found in Boardman (2016), Fischer et al. (2018), Prasuhn (2020), and Van Oost et al.  
323 (2005). Rills underneath centre-pivots in Cristalina appear commensurate to gully  
324 networks, such as those developed in olive orchards in Spain (Castillo et al., 2012).

325 In some cases, the centre-pivot images illustrate widespread signs of soil erosion  
326 over a large proportion of the field, significantly impacting on crop production (Figure  
327 10).

328 The large field sizes found under the centre pivots is likely to be responsible for the  
329 length of the Cristalina rills exceeding those of Central Europe and the UK, where  
330 field sizes are much smaller and land use is much patchier. For example, a single  
331 centre-pivot in Cristalina can cover a larger area than the 94 ha experimental  
332 catchment where Cerdan et al. (2002) monitored rill erosion in multiple fields with 1 –  
333 10 ha.



334  
335 Figure 9. Stacked histogram of the longest rill lengths per centre-pivot field observed  
336 in the GE images for irrigated areas in Cristalina, Brazil.

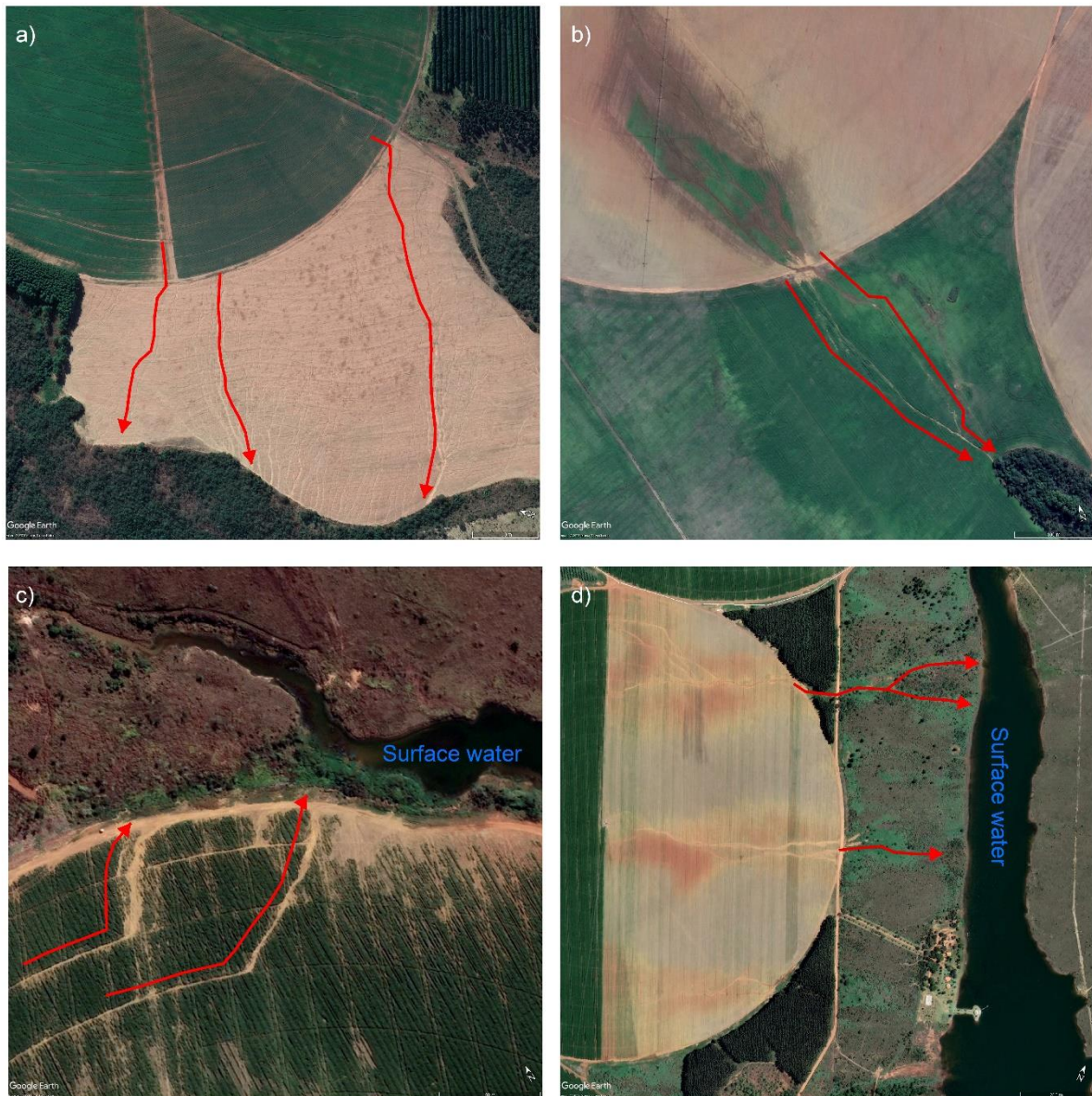




337

338 Figure 10. Severe signs of soil erosion over a large proportion of the centre-pivot field  
339 (Pivot ID 11508, diameter = 800 m), compromising crop yields in the affected area  
340 (about 30% of the field) (May 2020). Adjacent rainfed, terraced cropland on the right  
341 side of the image does not show similar erosional features. Imagery from Google  
342 Earth™.

343 The analysed images also indicate off-site erosion impacts. Runoff from the centre-  
344 pivot fields flows downslope into adjacent fields, even during the dry season (Figure  
345 11a). Moreover, the concentrated flow from within the centre-pivot irrigated areas  
346 sometimes crosses adjacent roads and field boundaries, creating rill channels across  
347 downslope fields (Figure 11b). Additionally, we observed soil erosion off-site effects  
348 associated to the runoff connectivity to surface waters (Figure 11c,d). Since runoff  
349 from agricultural land is often linked to the transport of particulate and dissolved  
350 pollutants (Didoné et al., 2021; Quinton and Catt, 2007), the overland flow originating  
351 from underneath centre-pivots and moving into surface waters poses a threat to  
352 water quality and supply in Cristalina.



353

354 Figure 11. a) Extensive erosion in a fallow field downslope from a centre pivot (Pivot  
 355 ID 12214, diameter = 930 m) during the dry season (July 2018): rills initiate along the  
 356 flow paths from the irrigated upslope field. b) Erosion rills starting from the outflow of  
 357 a grassed waterway of a centre-pivot field (Pivot ID 11816, diameter = 1100 m) and  
 358 cutting through a downslope rainfed field until reaching a woodland (May 2020). c)  
 359 Eroding centre-pivot field (Pivot ID 11697, diameter = 1230 m) close to surface water:  
 360 rills initiate from breached centre-pivot-wheel tracks and flow downslope towards the  
 361 stream network (June 2021). d) Runoff path downstream from an eroding centre-

362 pivot field (Pivot ID 11685, diameter = 1240 m) connecting with surface water (April  
363 2018). Imagery from Google Earth™.

364 Regarding the causes of soil erosion in the centre-pivot irrigated fields, we found that  
365 rill incision was often linked to centre-pivot-wheel tracks (e.g., Figures 11c, 8b,d),  
366 which were identified as the direct cause for rill development in at least 51 centre-  
367 pivot-field images. These tracks can undergo severe compaction if the lateral tower is  
368 moving over ponded or saturated soil, creating deep circular channels that intercept  
369 runoff within the irrigated fields (Kincaid, 2002) (Figure 12). We identified that rill  
370 incision occurred as these circular channels collected runoff and sediment along the  
371 flow path, until reaching a point in which the topographical flow direction becomes  
372 perpendicular to the tangent of circular wheel track. At this stage, the concentrated  
373 flow breaks through the compacted wheel-channel banks (Figure 11c). The rill may  
374 also cross parallel tracks, where it might receive runoff and sediment from that track,  
375 creating a highly connected rill network (Figure 8d).



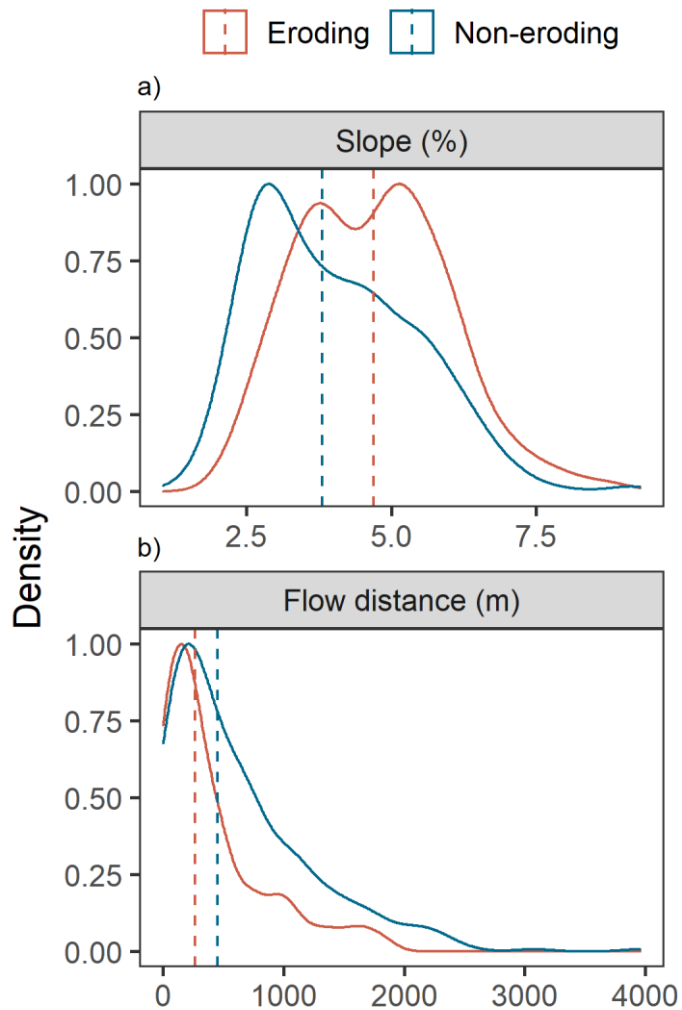


376

377 Figure 12. A centre-pivot wheel creating a compacted track as it moves over wet soil  
378 with surface ponding in Macaia, Minas Gerais, Brazil. Photo from Victor B. S.  
379 Baptista.

380 The DEM-extracted terrain attributes from the centre-pivot fields further allow us to  
381 draw conclusions about the locations of the eroding centre pivots: (i) eroding centre-  
382 pivot fields were located in areas with higher slopes than the fields without erosion  
383 features (median slope for eroding fields = 4.7%, median for non-eroding fields =  
384 3.8%, Figure 13); (ii) the eroding fields had shorter distances along the flow path to  
385 the nearest stream channels (median = 263 m, Figure 13) compared to the non-  
386 eroding (median = 452 m, Figure 13), indicating the incision of erosion rills in flow-  
387 accumulating, convex positions of the landscape.



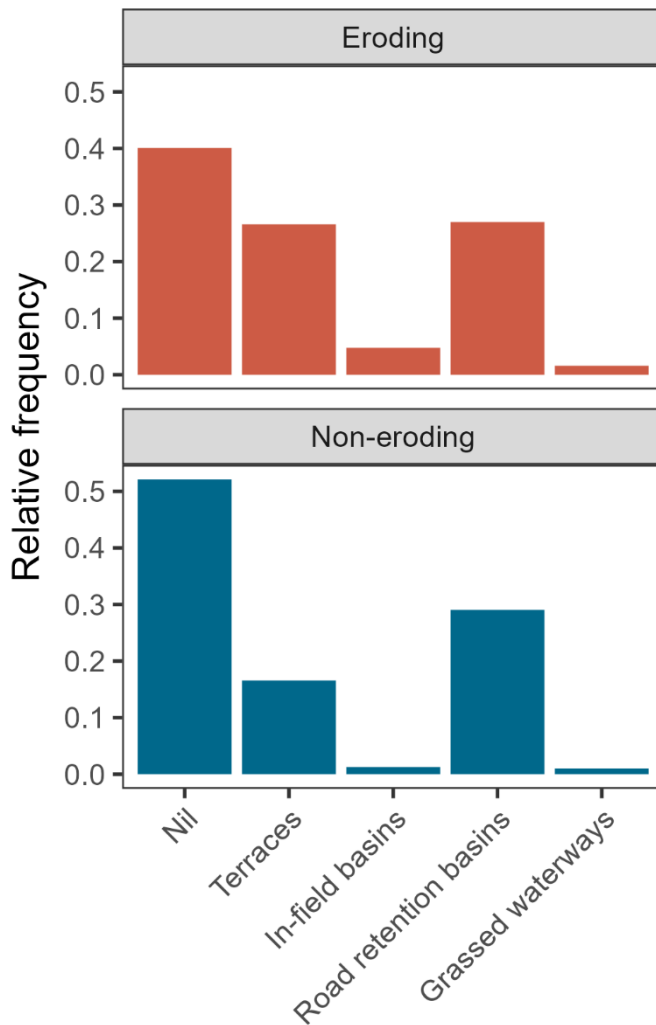


388

389 Figure 13. Scaled probability density function of the mean slope (%) per centre-pivot  
 390 field (a) and minimum flow distance to the nearest stream channel (m) per centre-  
 391 pivot field (b) in Cristalina, Brazil. Dashed lines represent group medians (eroding,  
 392 non-eroding).

393 The main soil conservation and offsite pollution control structures currently employed  
 394 in the centre-pivot fields were retention basins and broad-based terraces (Figure 14).  
 395 Of note is that soil conservation practices, particularly terracing, were more frequently  
 396 identified in the eroding centre-pivot fields, compared to the non-eroding (Figure 14).  
 397 This is possibly the result of terraces being established as a means to counteract soil  
 398 erosion, rather than preventing it. However, improvised terraces (i.e., not properly

399 designed along contour lines), seemed to be ineffective in stopping soil erosion once  
 400 rill channels were already incised (Figure 8c).



401

402 Figure 14. Relative frequency (0 – 1) of soil conservation and offsite pollution-control  
 403 structures observed in centre-pivot fields in Cristalina, Brazil.

404 **3.4 Perspectives for managing soil erosion in centre-pivot irrigated fields in the**  
 405 **Brazilian Cerrado**

406 The extent and severity of soil erosion features under centre-pivot irrigation systems  
 407 in Cristalina are leading to significant land degradation. Based on the analysis of  
 408 potential causes of soil erosion in the area, we can recommend some best-

409 management practices to control soil erosion and surface runoff in centre-pivot  
410 irrigated fields in the Brazilian Cerrado.

411 To address management challenges associated with centre-pivot irrigation, such as  
412 high water-application rates and the potential for wheel-track compaction, soil  
413 conservation practices that promote soil cover and soil water infiltration and prevent  
414 harmful runoff concentration during both irrigation and the summer-concentrated  
415 rainfall are required. These include zero tillage, reservoir tillage, broad-based  
416 terracing, retention basins, and grassed waterways (Fiener and Auerswald, 2003;  
417 Hörbe et al., 2021; Silva, 2017). Although zero-tillage is widely employed in the  
418 Brazilian Cerrado, this technique alone is not always sufficient to prevent soil erosion  
419 and combining it with other soil conservation practices, such as broad-based  
420 terracing, has been shown to be more effective (e.g., Didoné et al., 2017; Londero et  
421 al., 2021).

422 Adequate design and operation of centre-pivot systems are as important as soil  
423 management for preventing runoff and erosion during irrigation (Lehrsch et al., 2014).  
424 If properly managed, centre-pivot systems can be highly effective and have been  
425 shown to improve soil and surface water quality in areas where furrow irrigation was  
426 used previously (Bjorneberg et al., 2020; Ippolito et al., 2017). Booms (or offset  
427 booms or boom backs) on alternate sides of the centre-pivot lateral line are an  
428 effective approach for reducing water application rates by increasing the sprinkler  
429 wetted area (Nakawuka et al., 2014). Moreover, boom backs designed to extend the  
430 sprinklers behind centre-pivot wheels can keep wheel tracks dry until the lateral  
431 passage, which reduces the potential for tyre-rut formation (Martin et al., 2017). This  
432 is critical, as our results indicate that avoiding soil compaction on the centre-pivot-  
433 wheel tracks should be a priority. Variable-rate sprinklers can also help preventing

434 runoff by use of a variable discharge rate depending on field characteristics (Martin et  
435 al., 2017).

436 Ultimately, controlling soil erosion and surface runoff in centre-pivot irrigated fields in  
437 the Brazilian Cerrado is crucial to avoid the erosional effects that exacerbate crop  
438 vulnerability to droughts (Quinton et al., 2022). For instance, soil erosion by water  
439 selectively removes finer soil particles and soil organic carbon, reducing soil water  
440 holding capacity and increasing runoff propensity (Batista et al., 2023b). Hence,  
441 erosion is likely to increase irrigation demands, as a lesser proportion of the  
442 precipitation becomes eventually available to plants, creating a highly undesirable  
443 positive feedback loop between irrigation and soil erosion.

#### 444 **4 Conclusions**

445 Here we have used Google Earth™ (GE) images to map erosion features for 738  
446 centre-pivot fields (total area = 56 462 ha) in the municipality of Cristalina, in the  
447 Brazilian Cerrado. We found that:

- 448 i) at least 29% of centre-pivot fields in the study area displayed signs of rill  
449 erosion over the latest five available GE images at the time of the analysis  
450 (median image year per centre-pivot = 2019, median image range per centre-  
451 pivot = 3 years),
- 452 ii) rills were mostly identified during the dry season, which coincided with time of  
453 the year of greater image availability, and
- 454 iii) the median length of the longest rill per centre-pivot field was 260 m, with  
455 maximum values over 1200 m.

456 The consistent identification of widespread, severe erosion features underneath the  
457 centre-pivots during the dry season of the Brazilian Cerrado strongly suggests that

458 irrigation causes or aggravates erosion in the study area. Our analysis further  
459 demonstrated how centre-pivot irrigation can directly cause soil erosion, due to  
460 excessive application rates in periods of very low rainfall; or indirectly, due to the  
461 creation of circular pivot-wheel-track channels that are breached in flow-accumulating  
462 convexities and promote rill initiation. Furthermore, we found that eroding centre-pivot  
463 fields in Cristalina were more likely to be found in the proximity of surface waters,  
464 which increases the risk of sediment and pollutant delivery to water courses.

465 To the best of our knowledge, this is the first systematic report of widespread and  
466 severe soil erosion under centre-pivot irrigated fields worldwide. As centre-pivots are  
467 already the preferred irrigation method for many important crop-growing regions in  
468 the world and their use currently expanding to many other areas, our contribution  
469 raises a timely concern about the sustainability of current practices in centre-pivot  
470 irrigation. Although the potential for soil erosion underneath centre pivots has been  
471 recognised for some time, our results demonstrate how this can indeed be a serious,  
472 systematic issue in areas without appropriate soil and irrigation management.

#### 473 **5 CRediT authorship contribution statement**

474 PVGB: Conceptualisation, Methodology, Formal analysis, Investigation, Visualisation,  
475 Writing – Original Draft Preparation. VBSB: Conceptualisation, Investigation. FW:  
476 Methodology, Investigation, Writing – Reviewing and Editing. KS: Methodology,  
477 Investigation. JNQ: Writing – Reviewing and Editing, Supervision. PF: Writing –  
478 Reviewing and Editing, Supervision.

#### 479 **6 Declaration of competing interests**

480 The authors declare no competing interests.

#### 481 **7 Acknowledgements**

482 We acknowledge the use of Google Earth™ imagery ©2023 Google for figures 3, 8,  
483 10, and 11. Pedro V G Batista was supported by German Federal Ministry of Food  
484 and Agriculture (Grant No. 28DK118B20). The cooperation between Brazilian and  
485 Bavarian research institutions was supported by the Bavarian Academic Centre for  
486 Latin America (BAYLAT).

## 487 **8 Data accessibility statement**

488 The Google Earth™ images used in this research are free to access and available  
489 from Google Earth Pro on Desktop ([https://www.google.com/earth/versions/#earth-](https://www.google.com/earth/versions/#earth-pro)  
490 [pro](https://www.google.com/earth/versions/#earth-pro)). The digital elevation model used for the terrain analysis can be downloaded  
491 freely from the USGS Earth Explorer (<https://earthexplorer.usgs.gov/>). The centre-  
492 pivot shapefile from the Brazilian Irrigation Atlas is available at:  
493 [https://metadados.snirh.gov.br/geonetwork/srv/api/records/e2d38e3f-5e62-41ad-](https://metadados.snirh.gov.br/geonetwork/srv/api/records/e2d38e3f-5e62-41ad-87ab-990490841073)  
494 [87ab-990490841073](https://metadados.snirh.gov.br/geonetwork/srv/api/records/e2d38e3f-5e62-41ad-87ab-990490841073). The results from the erosion classification per centre-pivot field  
495 were uploaded to a data repository and are available at:  
496 <https://doi.org/10.5281/zenodo.7680625> (Batista et al., 2023a).

497

498 **References**

- 499 Aimar, F., Martínez-Romero, Á., Salinas, A., Giubergia, J.P., Severina, I., Marano,  
500 R.P., 2022. A revised equation of water application efficiency in a center pivot  
501 system used in crop rotation in no tillage. *Agronomy* 12, 2842.  
502 <https://doi.org/10.3390/agronomy12112842>
- 503 Alvares, C.A., Stape, J.L., Sentelhas, P.C., De Moraes Gonçalves, J.L., Sparovek,  
504 G., 2013. Köppen's climate classification map for Brazil. *Meteorol. Zeitschrift* 22,  
505 711–728. <https://doi.org/10.1127/0941-2948/2013/0507>
- 506 ANA – Agência Nacional de Águas e Saneamento Básico, 2021. Atlas Irrigação. Uso  
507 da água na agricultura irrigada, 2nd ed, Agência Nacional de Águas e  
508 Saneamento Básico. ANA, Brasília.
- 509 Baptista, V.B. da S., Córcoles, J.I., Colombo, A., Moreno, M.Á., 2019. Feasibility of  
510 the use of variable speed drives in center pivot systems installed in plots with  
511 variable topography. *Water (Switzerland)* 11, 2192.  
512 <https://doi.org/10.3390/w11102192>
- 513 Barcelos, A.A., Cassol, E.A., Denardin, J.E., 1999. Infiltração de água em um  
514 Latossolo vermelho-escuro sob condições de chuva intensa em diferentes  
515 sistemas de manejo. *Rev. Bras. Ciência do Solo* 23, 35–43.  
516 <https://doi.org/10.1590/s0100-06831999000100005>
- 517 Batista, P.V.G., Davies, J., Silva, M.L.N., Quinton, J.N., 2019. On the evaluation of  
518 soil erosion models : Are we doing enough ? *Earth-Science Rev.* 197, 102898.  
519 <https://doi.org/10.1016/j.earscirev.2019.102898>
- 520 Batista, P.V.G., Baptista, V. B. da S., Wilken, F., Seufferheld, K., Quinton, J.N.,  
521 Fiener, P., 2023a. Erosion-classification data for centre-pivot-irrigated fields in

522 Cristalina, Brazil. Zenodo. <https://doi.org/10.5281/zenodo.7680625>. [dataset]

523 Batista, P.V.G., Evans, D.L., Cândido, B.M., Fiener, P., 2023b. Does soil thinning  
524 change soil erodibility? An exploration of long-term erosion feedback systems.  
525 SOIL 9, 71–88. <https://doi.org/10.5194/soil-9-71-2023>

526 Bjerneberg, D.L., Ippolito, J.A., King, B.A., Nouwakpo, S.K., Koehn, A.C., 2020.  
527 Moving toward sustainable irrigation in a southern idaho irrigation project. Trans.  
528 ASABE 63, 1441–1449. <https://doi.org/10.13031/TRANS.13955>

529 Boardman, J., 2016. The value of Google Earth™ for erosion mapping. Catena 143,  
530 123–127. <https://doi.org/10.1016/j.catena.2016.03.031>

531 Boardman, J., Evans, R., 2020. The measurement, estimation and monitoring of soil  
532 erosion by runoff at the field scale: Challenges and possibilities with particular  
533 reference to Britain. Prog. Phys. Geogr. 44, 31–49.  
534 <https://doi.org/10.1177/0309133319861833>

535 Castillo, C., Pérez, R., James, M.R., Quinton, J.N., Taguas, E. V., Gómez, J.A.,  
536 2012. Comparing the accuracy of several field methods for measuring gully  
537 erosion. Soil Sci. Soc. Am. J. 76, 1319. <https://doi.org/10.2136/sssaj2011.0390>

538 Cerdan, O., Le Bissonnais, Y., Couturier, A., Bourennane, H., Souchère, V., 2002.  
539 Rill erosion on cultivated hillslopes during two extreme rainfall events in  
540 Normandy, France. Soil Tillage Res. 67, 99–108. [https://doi.org/10.1016/S0167-](https://doi.org/10.1016/S0167-1987(02)00045-4)  
541 [1987\(02\)00045-4](https://doi.org/10.1016/S0167-1987(02)00045-4)

542 Didoné, E.J., Minella, J.P.G., Evrard, O., 2017. Measuring and modelling soil erosion  
543 and sediment yields in a large cultivated catchment under no-till of Southern  
544 Brazil. Soil Tillage Res. 174, 24–33. <https://doi.org/10.1016/j.still.2017.05.011>



545 Didoné, E.J., Minella, J.P.G., Tiecher, T., Zanella, R., Prestes, O.D., Evrard, O.,  
546 2021. Mobilization and transport of pesticides with runoff and suspended  
547 sediment during flooding events in an agricultural catchment of Southern Brazil.  
548 Environ. Sci. Pollut. Res. 28, 39370–39386. [https://doi.org/10.1007/s11356-021-](https://doi.org/10.1007/s11356-021-13303-z)  
549 13303-z

550 EMATER – Agência Goiana de Assistência Técnica, Extensão Rural e Pesquisa  
551 Agropecuária, 2016. Distribuição dos solos de Goiás (1:250 000). Accessed 31  
552 Augst 2022. <<http://www.sieg.go.gov.br/siegdownloads/>>

553 Fiener, P., Auerswald, K., 2003. Effectiveness of grassed waterways in reducing  
554 runoff and sediment delivery from agricultural watersheds. J. Environ. Qual. 32,  
555 927–936. <https://doi.org/10.2134/jeq2003.9270>

556 Fischer, F.K., Kistler, M., Brandhuber, R., Maier, H., Treisch, M., Auerswald, K.,  
557 2018. Validation of official erosion modelling based on high-resolution radar rain  
558 data by aerial photo erosion classification. Earth Surf. Process. Landforms 43,  
559 187–194. <https://doi.org/10.1002/esp.4216>

560 Garrett, R.D., Koh, I., Lambin, E.F., le Polain de Waroux, Y., Kastens, J.H., Brown,  
561 J.C., 2018. Intensification in agriculture-forest frontiers: Land use responses to  
562 development and conservation policies in Brazil. Glob. Environ. Chang. 53, 233–  
563 243. <https://doi.org/10.1016/j.gloenvcha.2018.09.011>

564 Gilley, J.R., 1984. Suitability of Reduced Pressure Center-Pivots. J. Irrig. Drain. Eng.  
565 110, 22–34. [https://doi.org/10.1061/\(asce\)0733-9437\(1984\)110:1\(22\)](https://doi.org/10.1061/(asce)0733-9437(1984)110:1(22))

566 Gulhati, N.D., Smith, W.C., 1967. Irrigated agriculture: An historical review, in:  
567 Hagan, R.M., Haise, H.R., Edminster, T.W. (Eds.), Irrigation of Agricultural  
568 Lands. American Society of Agronomy, Madison, pp. 3–11.

569 <https://doi.org/10.2134/agronmonogr11.c1>

570 Hasheminia, S.M., 1994. Controlling runoff under low pressure center pivot irrigation  
571 systems. *Irrig. Drain. Syst.* 8, 25–34. <https://doi.org/10.1007/BF00880796>

572 Hörbe, T., Minella, J.P.G., Schneider, F.J.A., Londero, A.L., Gubiani, P.I., Merten,  
573 G.H., Schlesner, A., 2021. Managing runoff in rainfed agriculture under no-till  
574 system: Potential for improving crop production. *Rev. Bras. Cienc. do Solo* 45,  
575 1–17. <https://doi.org/10.36783/18069657rbcs20210015>

576 Hunke, P., Mueller, E.N., Schröder, B., Zeilhofer, P., 2015. The Brazilian Cerrado:  
577 Assessment of water and soil degradation in catchments under intensive  
578 agricultural use. *Ecohydrology* 8, 1154–1180. <https://doi.org/10.1002/eco.1573>

579 IBGE – Instituto Brasileiro de Geografia e Estatística, 2017. Censo agropecuário de  
580 2017. Accessed 26 November 2022.  
581 <<https://cidades.ibge.gov.br/brasil/go/cristalina/pesquisa/24/27745> >.

582 Ippolito, J.A., Bjorneberg, D., Stott, D., Karlen, D., 2017. Soil quality improvement  
583 through conversion to sprinkler irrigation. *Soil Sci. Soc. Am. J.* 81, 1505–1516.  
584 <https://doi.org/10.2136/sssaj2017.03.0082>

585 Johansen, K., Lopez, O., Tu, Y.H., Li, T., McCabe, M.F., 2021. Center pivot field  
586 delineation and mapping: A satellite-driven object-based image analysis  
587 approach for national scale accounting. *ISPRS J. Photogramm. Remote Sens.*  
588 175, 1–19. <https://doi.org/10.1016/j.isprsjprs.2021.02.019>

589 Kincaid, D.C., 2005. Application rates from center pivot irrigation with current  
590 sprinkler types. *Appl. Eng. Agric.* 21, 605–610.

591 Kincaid, D.C., 2002. The WEPP model for runoff and erosion prediction under

592           sprinkler irrigation. *Trans. ASAE* 45, 67–72. <https://doi.org/10.13031/2013.7875>

593 Kincaid, D.C., McCann, I., Bush, J.R., Hasheminia, M., 1990. Low pressure center  
594           pivot irrigation and reservoir tillage, in: *Visions of the Future, Proceedings of the*  
595           Third National Irrigation Symposium. American Society of Agricultural  
596           Engineers, pp. 54–60.

597 King, B.A., 2016. Moving spray-plate center-pivot sprinkler rating index for assessing  
598           runoff potential. *Trans. ASABE* 59, 225–237.  
599           <https://doi.org/10.13031/trans.59.11162>

600 King, B.A., Bjorneberg, D.L., 2011. Evaluation of potential runoff and erosion of four  
601           center pivot irrigation sprinklers. *Appl. Eng. Agric.* 27, 75–85.  
602           <https://doi.org/10.13031/2013.36226>

603 Lehrs, G.A., Lentz, R.D., Bjorneberg, D.L., Sojka, R.E., 2014. Irrigation-induced,  
604           Reference module in earth systems and environmental sciences. Elsevier Inc.  
605           <https://doi.org/10.1016/b978-0-12-409548-9.09019-9>

606 Lian, J., Li, Yulin, Li, Yuqiang, Zhao, X., Zhang, T., Wang, Xinyuan, Wang, Xuyang,  
607           Wang, L., Zhang, R., 2022. Effect of center-pivot irrigation intensity on  
608           groundwater level dynamics in the agro-pastoral ecotone of Northern China.  
609           *Front. Environ. Sci.* 10, 1–12. <https://doi.org/10.3389/fenvs.2022.892577>

610 Londero, A.L., Minella, J.P.G., Schneider, F.J.A., Deuschle, D., Merten, G.H., Evrard,  
611           O., Boeni, M., 2021. Quantifying the impact of no-till on sediment yield in  
612           southern Brazil at the hillslope and catchment scales. *Hydrol. Process.* 35, 1–16.  
613           <https://doi.org/10.1002/hyp.14286>

614 Lopes, A.S., Guilherme, L.R.G., 2016. A career perspective on soil management in  
615           the Cerrado region of Brazil, *Advances in Agronomy*. Elsevier Inc.

616 <https://doi.org/10.1016/bs.agron.2015.12.004>

617 Marques, J.J., Schulze, D.G., Curi, N., Mertzman, S.A., 2004. Major element  
618 geochemistry and geomorphic relationships in Brazilian Cerrado soils.  
619 *Geoderma* 119, 179–195. [https://doi.org/10.1016/S0016-7061\(03\)00260-X](https://doi.org/10.1016/S0016-7061(03)00260-X)

620 Martin, D., Kranz, W.L., Smith, T., Irmak, S., Burr, C., Yoder, R., 2017. Center pivot  
621 irrigation handbook. University of Nebraska-Lincoln, Lincoln.

622 Nakawuka, P., Okwany, R.O., Peters, R.T., Desta, K., Sadeghi, S.H., 2014. Efficacy  
623 of boom systems in controlling runoff under center pivots and linear move  
624 irrigation systems. *Appl. Eng. Agric.* 30, 797–801.  
625 <https://doi.org/10.13031/aea.30.10540>

626 Panachuki, E., Bertol, I., Sobrinho, T.A., de Oliveira, P.T.S., Rodrigues, D.B.B., 2011.  
627 Soil and water loss and water infiltration in red latosol under different  
628 management systems. *Rev. Bras. Cienc. do Solo* 35, 1777–1785.  
629 <https://doi.org/10.1590/s0100-06832011000500032>

630 Phocaides, A., 2000. Technical handbook on pressurized irrigation techniques. FAO,  
631 Rome.

632 Prasuhn, V., 2020. Twenty years of soil erosion on-farm measurement: annual  
633 variation, spatial distribution and the impact of conservation programmes for soil  
634 loss rates in Switzerland. *Earth Surf. Process. Landforms* 45, 1539–1554.  
635 <https://doi.org/10.1002/esp.4829>

636 Puy, A., Lo Piano, S., Saltelli, A., 2020. Current models underestimate future irrigated  
637 areas. *Geophys. Res. Lett.* 47, 1–10. <https://doi.org/10.1029/2020GL087360>

638 Quinton, J.N., Catt, J.A., 2007. Enrichment of heavy metals in sediment resulting

639 from soil erosion on agricultural fields. *Environ. Sci. Technol.* 41, 3495–3500.  
640 <https://doi.org/10.1021/es062147h>

641 Quinton, J.N., Öttl, L.K., Fiener, P., 2022. Tillage exacerbates the vulnerability of  
642 cereal crops to drought. *Nat. Food* 3, 472–479. [https://doi.org/10.1038/s43016-](https://doi.org/10.1038/s43016-022-00533-8)  
643 [022-00533-8](https://doi.org/10.1038/s43016-022-00533-8)

644 Rosa, L., 2022. Adapting agriculture to climate change via sustainable irrigation:  
645 Biophysical potentials and feedbacks. *Environ. Res. Lett.* 17, 063008.  
646 <https://doi.org/10.1088/1748-9326/ac7408>

647 Saggau, P., Kuhwald, M., Hamer, W.B., Duttman, R., 2022. Are compacted  
648 tramlines underestimated features in soil erosion modeling? A catchment-scale  
649 analysis using a process-based soil erosion model. *L. Degrad. Dev.* 33, 452–  
650 469. <https://doi.org/10.1002/ldr.4161>

651 Siebert, S., Kummu, M., Porkka, M., Döll, P., Ramankutty, N., Scanlon, B.R., 2015. A  
652 global data set of the extent of irrigated land from 1900 to 2005. *Hydrol. Earth*  
653 *Syst. Sci.* 19, 1521–1545. <https://doi.org/10.5194/hess-19-1521-2015>

654 Silgram, M., Jackson, D.R., Bailey, A., Quinton, J., Stevens, C., 2010. Hillslope scale  
655 surface runoff, sediment and nutrient losses associated with tramline wheelings.  
656 *Earth Surf. Process. Landforms* 35, 699–706. <https://doi.org/10.1002/esp.1894>

657 Silva, L.L., 2017. Are basin and reservoir tillage effective techniques to reduce runoff  
658 under sprinkler irrigation in Mediterranean conditions? *Agric. Water Manag.* 191,  
659 50–56. <https://doi.org/10.1016/j.agwat.2017.06.003>

660 Silva, L.L., 2006. The effect of spray head sprinklers with different deflector plates on  
661 irrigation uniformity, runoff and sediment yield in a Mediterranean soil. *Agric.*  
662 *Water Manag.* 85, 243–252. <https://doi.org/10.1016/j.agwat.2006.05.006>

663 Van Oost, K., Govers, G., Cerdan, O., Thauré, D., Van Rompaey, a., Steegen, a.,  
664 Nachtergaele, J., Takken, I., Poesen, J., 2005. Spatially distributed data for  
665 erosion model calibration and validation: The Ganspoel and Kinderveld datasets.  
666 *Catena* 61, 105–121. <https://doi.org/10.1016/j.catena.2005.03.001>

667 Wang, X., Müller, C., Elliot, J., Mueller, N.D., Ciais, P., Jägermeyr, J., Gerber, J.,  
668 Dumas, P., Wang, C., Yang, H., Li, L., Deryng, D., Folberth, C., Liu, W.,  
669 Makowski, D., Olin, S., Pugh, T.A.M., Reddy, A., Schmid, E., Jeong, S., Zhou,  
670 F., Piao, S., 2021. Global irrigation contribution to wheat and maize yield. *Nat.*  
671 *Commun.* 12, 1–8. <https://doi.org/10.1038/s41467-021-21498-5>

672 Zweifel, L., Meusburger, K., Alewell, C., 2019. Spatio-temporal pattern of soil  
673 degradation in a Swiss Alpine grassland catchment. *Remote Sens. Environ.* 235,  
674 111441. <https://doi.org/10.1016/j.rse.2019.111441>

675

**Declaration of interests**

The authors declare that they have no known competing financial interests or personal relationships that could have appeared to influence the work reported in this paper.

The authors declare the following financial interests/personal relationships which may be considered as potential competing interests:

**CRedit authorship contribution statement**

PVGB: Conceptualisation, Methodology, Formal analysis, Investigation, Visualisation, Writing – Original Draft Preparation. VBSB: Conceptualisation, Investigation. FW: Methodology, Investigation, Writing – Reviewing and Editing. KS: Methodology, Investigation. JNQ: Writing – Reviewing and Editing, Supervision. PF: Writing – Reviewing and Editing, Supervision.